

# Nano-Structured 7YSZ Electrolyte Layer for Solid Oxide Fuel Cell Prepared by Plasma Spray-Physical Vapor Deposition

Xu Wei<sup>1,2</sup>, Zhang Xiaofeng<sup>2</sup>, Zhou Kesong<sup>1,2</sup>, Niu Shaopeng<sup>2</sup>, Chang Fa<sup>3</sup>, Liu Min<sup>2</sup>,  
Deng Chunming<sup>2</sup>, Deng Ziqian<sup>2</sup>

<sup>1</sup> Central South University, Changsha 410083, China; <sup>2</sup> National Engineering Laboratory for Modern Materials Surface Engineering Technology, The Key Lab of Guangdong for Modern Surface Engineering Technology, Guangdong Institute of New Materials, Guangzhou 510650, China; <sup>3</sup> Fujian University of Technology, Fuzhou 350118, China

**Abstract:** Due to high thermal stability and pure oxide ionic conductivity, yttria-stabilized zirconia (YSZ) is the most commonly used electrolyte material for solid oxide fuel cell (SOFC). Nano-structured 7YSZ electrolyte layers were fabricated by plasma spray-physical vapor deposition (PS-PVD) system. The micrograph, microstructure, mechanical properties and gas permeability were characterized by SEM, TEM, 3D X-ray CT and nano-indenter. Moreover, the deposition mechanism of PS-PVD was also discussed. Results indicate that 7YSZ electrolyte layers with a thickness of 8.7~12.3  $\mu\text{m}$  were successfully prepared. The substrate temperature is a key factor to form this advanced structure controlled at  $\sim 600$  °C. The gas permeability of the nano-structured 7YSZ electrolyte layer can achieve  $2.24 \times 10^{-8} \sim 2.29 \times 10^{-8} \text{ cm}^4 \cdot \text{gf}^{-1} \cdot \text{s}^{-1}$ . It also shows good mechanical properties, of which the recovery rate, hardness and elastic modulus are 57%, 10 GPa and 140 GPa, respectively.

**Key words:** SOFC; YSZ; PS-PVD; electrolyte layer

In recent years the research and development on intermediate temperature solid oxide fuel cells (IT-SOFC) with an operating temperature of 400~700 °C has emerged as one of the active areas of investigations<sup>[1,2]</sup>. IT-SOFC provides a greater flexibility in the fabrication of electrodes, cell interconnectors and results in reduced thermal degradation and thermal cycling stress. However, lowering of the operating temperature of SOFC necessitates considerable reduction in thickness (to a few microns) of the conventionally used electrolytes such as yttria stabilized zirconia (YSZ) to minimize the ohmic losses<sup>[3,4]</sup>. Besides, fabrication of nano-structured electrolyte layer is also a tendency to improve the operation performance<sup>[5,6]</sup>. Though thin layer electrolytes could well be fabricated by traditional techniques such as tape casting<sup>[5,7]</sup>, atmospheric plasma spraying (APS)<sup>[8-10]</sup>, etc., these techniques are difficult to obtain a nano-structured thin electrolyte layer.

The present work is intended to explore the possibility of

fabricating dense thin electrolyte layer with nano-structure. It is hard to prepare nano-structured layer by conventional technique APS because nano-agglomerated powder injected into plasma gun will grow into micro-grains<sup>[10,11]</sup>. Tape casting is as a universal method to prepared dense electrolytes layer. Due to high sintering temperature ( $>1300$  °C), the nano-sized powders in slurry after casting will grow<sup>[7,12]</sup>. Thus, in the present investigation, there is a novel technique for SOFC fabrication by employing plasma spray-physical vapor deposition (PS-PVD).

The PS-PVD was named for vapor phase deposition through using plasma spray. The PS-PVD process has been developed with the aim of depositing different structured functional coatings, such as thin, gas tight and columnar coating with large area coverage by plasma spray<sup>[10,13-15]</sup>. The PS-PVD is developed based on low pressure plasma spray (LPPS), where electrical current up to 3000 A and plasma gas

Received date: December 12, 2018

Foundation item: National Key Research and Development Program of China (2017YFB0306100); Guangdong Academy of Sciences Program (2017GDASCX-0202, 2018GDASCX-0402, 2018GDASCX-0111); Guangdong Technical Research Program (2017B090916002, 2017A070701027); Guangdong Natural Science Foundation (2016A030312015, 2017A030310315); Guangzhou Technical Research Program (201605131008557, 201707010385)

Corresponding author: Zhang Xiaofeng, Ph. D., Guangdong Institute of New Materials, Guangzhou 510650, P. R. China, E-mail: zxf200808@126.com

Copyright © 2019, Northwest Institute for Nonferrous Metal Research. Published by Science Press. All rights reserved.

flow up to 200 L/min, an input power level of 180 kW could be achieved. With the operation pressure decreasing ( $\sim 100$  Pa), the plasma plume expands to a length of more than 2200 mm and 400 mm in diameter<sup>[16]</sup>. Using appropriate parameters, it is possible to evaporate the powder feedstock materials to obtain dense nano-structured thin electrolyte layer.

## 1 Experiment

The facility used in the experiment is PS-PVD multicoat system (Oerlikon Metco), which was obtained by reconstruction of a conventional LPPS system. By the addition of a large vacuum blower, the pumping capacity at the PS-PVD working pressure of 50~200 Pa was enhanced. And the electrical input power was up to 180 kW. For PS-PVD operation, a modified single cathode O3CP gun was used. The feedstock material was an agglomerated 7YSZ designated as M6700 (Oerlikon Metco,  $d_{10}=2$   $\mu\text{m}$ ,  $d_{50}=10$   $\mu\text{m}$ ,  $d_{90}=19$   $\mu\text{m}$ ), shown in Fig.1. Disks made of porous stainless steel 430 (12.7 mm $\times$ 2 mm) were used as substrates. After cleaning the substrate, a 7YSZ thin layer with a thickness of 8.7~12.3  $\mu\text{m}$  was deposited by the PS-PVD, where the substrate temperature was controlled at  $\sim 600$   $^{\circ}\text{C}$ . During the 7YSZ layer preparation process, an additional oxygen flow of 2 L/min was used to prevent a loss of oxygen in the 7YSZ layer driven by the reducing condition in the low pressure plasma plume.

The microstructure of PS-PVD 7YSZ layer was characterized by field emission-scanning electron microscope (FESEM, Nova-Nano430, FEI) and transmission electron micro-

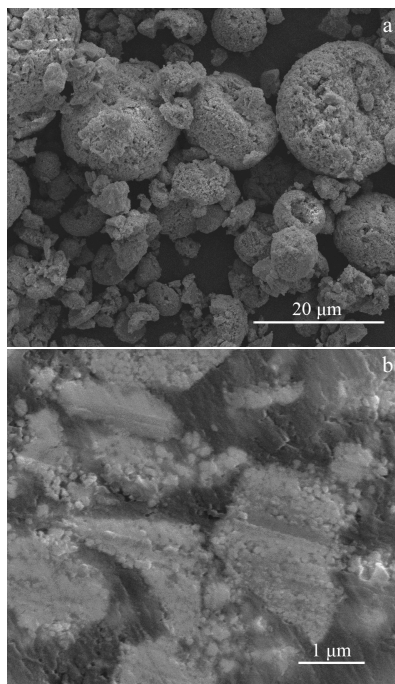


Fig.1 Morphologies of agglomerated 7YSZ powders before polishing (a) and after polishing (b)

scopy (TEM, Titan Themis 200, FEI) assisted with focused ion beam (FIB, 450S, FEI) milling. Moreover, micrographs of 7YSZ thin layer were observed by 3D X-ray CT (computed tomography, Xradia 410 Versa, ZEISS), where the volume resolution is 1  $\mu\text{m}$  and its operation voltage is 120 kV. The gas permeability of the as-sprayed electrolyte layer was measured. The effective area was evacuated by a vacuum pump. The pressure difference across the two sides of the sample was measured against the testing time after the evacuation was stopped. The gas permeability was easily calculated based on Darcy formula according the method described elsewhere. The effective thickness of the sample was considered to be equal to that of the electrolyte layer. The scheme of the tester for permeability is shown in Fig.2. The mechanical properties of 7YSZ electrolyte layers were evaluated by nano-indentation technique at a load of 3 mN. Nano-indentation tests were carried out using a nano-indenter (Hysitron, TI premier) with a Berkovich (tip radius $<150$  nm).

## 2 Results and Discussion

### 2.1 Nano-structured 7YSZ electrolyte layer preparation

7YSZ electrolyte layer was prepared by PS-PVD on porous stainless steel 430, as shown in Fig.3. Fig.3a and 3b indicate that dense thin layer with a thickness of 9.7~12.8  $\mu\text{m}$  can be obtained. As opposite to traditional APS technique, laminar-structured layer with apparent cracks and voids cannot be observed in PS-PVD layer. Through PS-PVD, the 7YSZ dense layer can be achieved on the surface with a hole, as indicated in Fig.3a. Besides, the interface between electrolyte layer and substrate is very dense, as shown in Fig.3b. Moreover, the microstructure of 7YSZ layer was characterized by TEM, as shown in Fig.4. Fig.4a is the bright field image of TEM slice filled by FIB, showing that the slice is closely packed by lots of nano-grains ( $<100$  nm). However, some voids are located in the slice. Magnified TEM image of slice shown in Fig.4b indicates the interfaces are dense among different-sized nano-grains. The gas permeability of the dense thin 7YSZ electrolyte layer was measured to be  $2.24 \times 10^{-8} \sim 2.29 \times 10^{-8} \text{ cm}^4 \cdot \text{gf}^{-1} \cdot \text{s}^{-1}$ , indicating that the 7YSZ electrolyte layer has a better gas tight performance than the APS 7YSZ electrolyte layer<sup>[10,17]</sup>.

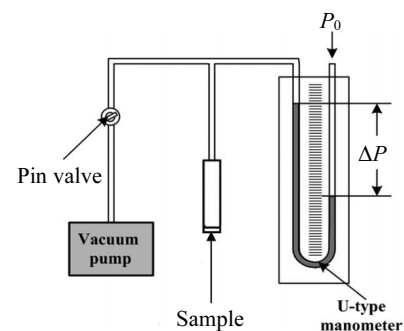


Fig.2 Schematic of the tester for gas permeability

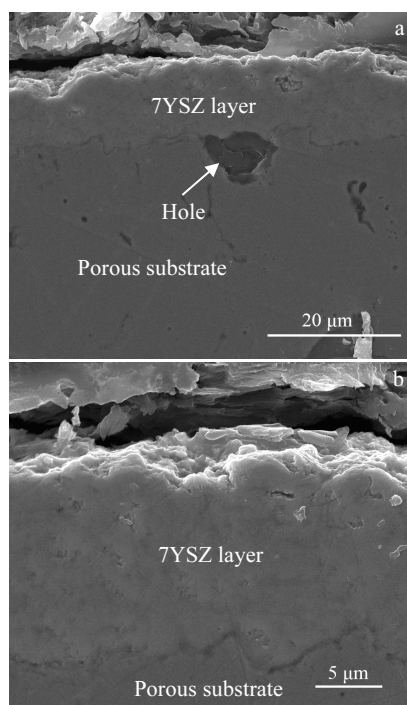


Fig.3 Cross-sectional microstructures of 7YSZ electrolyte layer on porous stainless steel 430

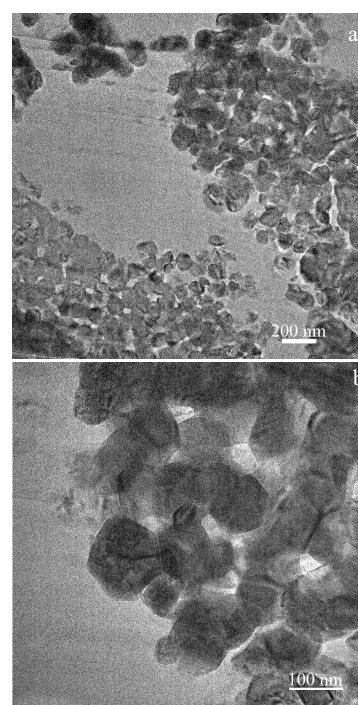


Fig.5 TEM micrographs of feedstock agglomerated 7YSZ powders before PS-PVD processing

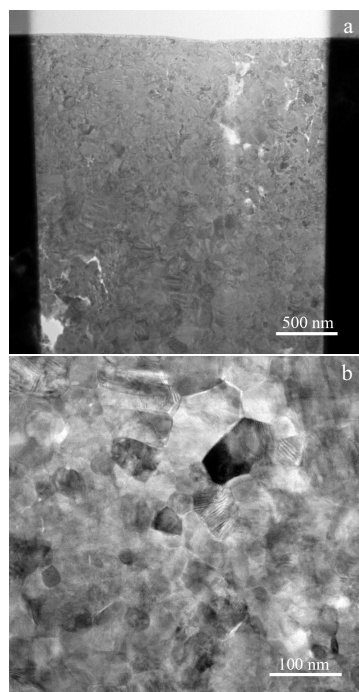


Fig.4 TEM micrographs of 7YSZ electrolyte layer

The TEM micrographs of feedstock agglomerated 7YSZ powders before PS-PVD processing are shown in Fig.5. The images show that the size of most grains is about 100 nm,

which are higher than the 7YSZ grain size in electrolyte layer (seen in Fig.4). In traditional techniques, such as APS, tape casting, using nano-structured powders as feedstock, due to high temperature in processing, the powders will grow into micro-sized grains. As opposite to the PS-PVD, in plasma gun, the powders can be evaporated due to high plasma power and low operation pressure to avoid grain growth<sup>[18,19]</sup>. Thus, the nano-structured 7YSZ electrolyte layer can be obtained by vapor deposition. On the contrary, the micro-structured electrolyte layer through APS was achieved because it was deposited by molten splat<sup>[17,20]</sup>.

## 2.2 Deposition mechanism of PS-PVD

Above results show that nano-structured 7YSZ electrolyte layer can be fabricated by PS-PVD due to vapor deposition. The transformation state of agglomerated 7YSZ powders in plasma jet is illustrated in Fig.6. Along with spray increasing in the direction of plasma jet flow, the state of 7YSZ powder will change gradually. During PS-PVD process, when the agglomerated 7YSZ powders are injected into plasma gun, the powders will separate into fine particles due to weak agglomeration of original particles<sup>[18]</sup>. At the beginning, the separated 7YSZ particles will transform from solid particles into liquid droplets in high temperature plasma gun. Subsequently the liquid 7YSZ droplets will be atomized into gas-droplet flow. Before reaching the substrate, most of atoms and ions are agglomerated into clusters. These clusters will nucleate and grow into nano-sized crystals once they impact

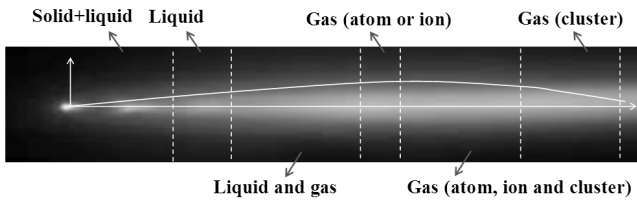


Fig.6 Photographs of PS-PVD plasma jet with 7YSZ powders injection

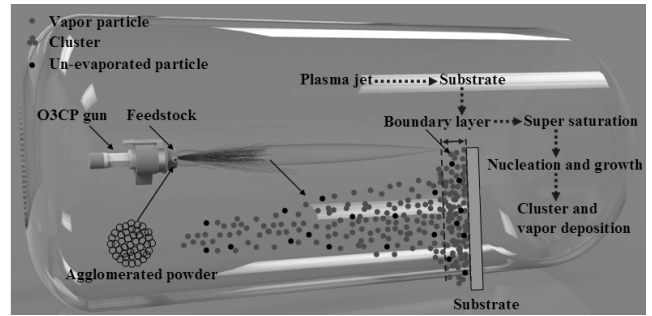


Fig.7 Schematic diagram of the nano-structured 7YSZ electrolyte layer deposited by PS-PVD

on the substrate. Finally, nano-structured 7YSZ electrolyte layer can be obtained, as shown in Fig.7.

Through above analysis of transformation state in plasma jet, a proposed deposition mechanism of nano-structured 7YSZ electrolyte layer in PS-PVD had been depicted in Fig.7. The agglomerated 7YSZ powders were injected into O3CP plasma gun and were accelerated and heated by high enthalpy plasma from the torch. The shape of particles plume is divergent, and thus high concentration of deposition species can be expected in the center of the plasma jet. In the PS-PVD chamber, the plasma jet is laminar. And the interaction between the plasma and surrounding atmosphere is weak<sup>[18-21]</sup>. Therefore, the velocity and temperature of the plasma jet cannot decrease quickly. When the hot plasma jet comes close to the relatively cool substrate, a boundary layer will be formed due to the rapid decrease of velocity and temperature generating temperature gradient<sup>[22-25]</sup>. Besides, in the boundary layer, lots of vapor particles impact the substrate and bounce back leading to a solubility gradient of vapor particle, which will generate a super-saturation status. Therefore, in parts of vapor particles, homogeneous nucleation will take place to form nano-sized cluster. The size of cluster is mainly dependent on the local concentration of vapor species and also influenced by cooling rate<sup>[25]</sup>. Meanwhile, in most of vapor particles, heterogeneous nucleation will take place directly on the substrate to form nano-grain dense packed microstructure. Both the homogeneous nucleation and the heterogeneous nucleation

contribute to the coating deposition and the microstructure of 7YSZ coating is mainly controlled by the substrate temperature<sup>[26]</sup>. In order to obtain a nano-structured layer, the substrate temperature was controlled at ~600 °C. If the substrate temperature increases to ~900 °C, columnar structured 7YSZ layer will be obtained.

**2.3 Characterization of 7YSZ electrolyte layer**

2D tomographies of 7YSZ electrolyte layer through X-ray CT are shown in Fig.8. The X-ray CT is a non-destructive technique, which is suitable to characterize thin layer because the X-ray can penetrate through the item easily. Using this method, the inner microstructure of 7YSZ electrolyte layer can be observed. Fig.8a is the image of the sample coated with electrolyte layer. Fig.8b~8d are the inner microstructures of electrolyte layer with different directions. Fig.8b shows that the 7YSZ can be deposited in cavity and shadow area through PS-PVD. Due to vapor deposition, non-line of sight deposition in PS-PVD is possible. Fig.8c and 8d show that electrolyte layer has high roughness and non-uniform thickness because of the layer deposited on a pot-holed porous substrate.

Mobility performance is an important factor for future commercial SOFC<sup>[27,28]</sup>. As a key component, physical mechanical property of 7YSZ electrolyte layer was characterized by nano-indentation test, as shown in Fig.9. Fig.9 indicates the

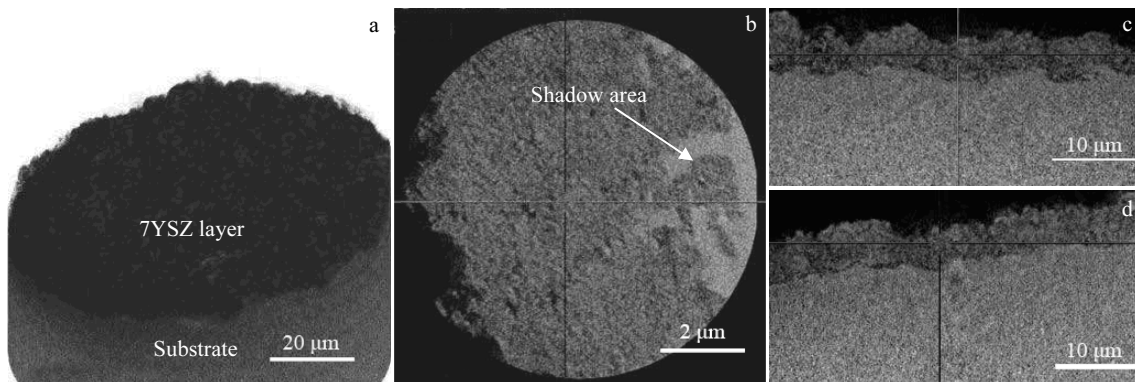


Fig.8 2D tomographies of 7YSZ electrolyte layer: (a) sample image and (b~d) different views of cross-sectional sample in Fig.8a

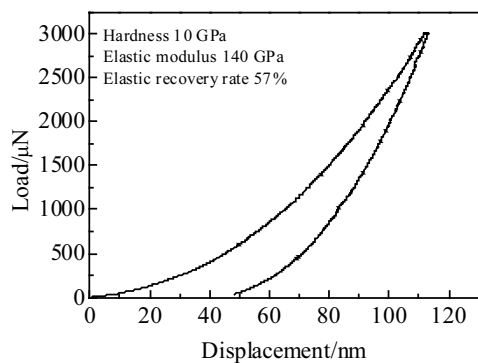


Fig.9 Loading-unloading curves of nano-structured 7YSZ

typical load-displacement curve obtained on the cross-section of the 7YSZ electrolyte layer. At the beginning, the loading curve shows linear variation indicating elastic deformation appearing in the electrolyte layer. But with the load increasing, the loading curve shows non-linear variation, which results from plastic deformation. In the un-loading process, the elastic deformation becomes recovery and the recovery rate is 57%. Besides, after calculation based on loading-unloading curve, the hardness and elastic modulus are 10 and 140 GPa, respectively. Thus, above results indicate that the 7YSZ electrolyte layer has a good balance on toughness and hardness due to its nano-structure. And the mechanical property of 7YSZ electrolyte layer prepared by PS-PVD is better than that of other electrolyte layer prepared by suspension plasma spray or sol-gel processing<sup>[29,30]</sup>.

### 3 Conclusions

1) Dense thin 7YSZ electrolyte layer with a thickness of 8.7~12.3 μm can be fabricated by PS-PVD on porous stain steel 430 and it has good bond with substrate. No laminar structure with crack and void was observed in the thin layer and its gas permeability was  $2.24 \times 10^{-8} \sim 2.29 \times 10^{-8} \text{ cm}^4 \cdot \text{gf}^{-1} \cdot \text{s}^{-1}$ .

2) The 7YSZ electrolyte layer has nano-structure, resulting from vapor deposition through PS-PVD. The substrate temperature is a key factor to form this advanced structure controlled at ~600 °C. Non-line of sight deposition can be achieved through PS-PVD. Thus, shadow area on porous substrate can be deposited.

3) Due to its nano-structure, the 7YSZ electrolyte layer has good mechanical properties characterized by nano-indentation. The recovery rate, hardness and elastic modulus are 57%, 10 GPa and 140 GPa, respectively.

### References

- Lu Junbiao, Zhang Zhongtai, Tang Zilong. *Rare Metal Materials and Engineering*[J], 2005, 34(8): 1177 (in Chinese)
- Wang Lishuang, Li Chengxin, Li Guangrong et al. *Journal of European Ceramic Society*[J], 2017, 37(15): 4751
- Pan Xia, Wu Yefan, Luo Linghong et al. *Rare Metal Materials and Engineering*[J], 2011, 40(S1): 310 (in Chinese)
- Hermawan E, Lee G S, Kim G S et al. *Ceramics International*[J], 2017, 43(13): 10 450
- Baquero T, Escobar J, Frade J et al. *Ceramics International*[J], 2013, 39(7): 8279
- Qiao Jinshuo, Sun Kening, Zhang Naiqing et al. *Rare Metal Materials and Engineering*[J], 2007, 36(S3): 113 (in Chinese)
- Nishihora R K, Rachadel P L, Quadri M G N et al. *Journal of European Ceramic Society*[J], 2018, 38(4): 988
- Prakash B S, Grips V K W, Aruna S T. *Journal of Power Sources*[J], 2014, 214: 358
- Wolf S, Adam R, Fuhrmann L et al. *Solid State Ionics*[J], 2013, 243: 30
- Marcano D, Mauer G, Vaßen R et al. *Surface and Coatings Technology*[J], 2017, 318: 170
- Zhang Xiaofeng, Zhou Kesong, Liu Min et al. *Ceramics International*[J], 2016, 42(16): 19 349
- Myung J, Ko H J, Park H G et al. *International Journal of Hydrogen Energy*[J], 2012, 37(1): 498
- Gindrat M, Höhle H M, Von Niessen K et al. *Journal of Thermal Spray*[J], 2011, 20: 882
- Zhang Xiaofeng, Zhou Kesong, Liu Min et al. *Surface and Coatings Technology*[J], 2015, 276: 316
- Lizuka K, Kambara M, Yoshida T. *Sensors and Actuators B: Chemical*[J], 2011, 155(2): 551
- Deng Ziqian, Liu Min, Mao Jie et al. *Vacuum*[J], 2017, 145: 39
- Zhang Shanlin, Li Chengxin, Li Changjiu. *Journal of Fuel Cell Science and Technology*[J], 2014, 11(3): 031 005
- Mauer G, Hospach A, Zotov N et al. *Journal of Thermal Spray Technology*[J], 2013, 22(2-3): 83
- Zhang Xiaofeng, Zhou Kesong, Liu Min et al. *Ceramics International*[J], 2018, 44(4): 3973
- Zhang Xiaofeng, Zhou Kesong, Xiao Xiaoling et al. *Materials Science Forum*[J], 2015, 816: 219
- Schmitt M P, Harder B J, Wolfe D E. *Surface and Coatings Technology*[J], 2016, 297: 11
- Zhang Xiaofeng, Zhou Kesong, Deng Chunming et al. *Journal of European Ceramic Society*[J], 2016, 36(3): 697
- Mauer G. *Plasma Chemistry and Plasma Processing*[J], 2014, 34(5): 1171
- Girshick S L, Chiu C P. *Plasma Chemistry and Plasma Processing*[J], 1989, 9(3): 355
- Liu Meijun, Zhang Meng, Zhang Qiang et al. *Journal of Thermal Spray Technology*[J], 2017, 26(7): 1641
- Deng Ziqian, Zhang Xiaofeng, Zhou Kesong et al. *Chinese Journal of Aeronautics*[J], 2018, 31(4): 820
- Dimitrova Z, Marechal F. *Renewable Energy*[J], 2017, 112: 124
- Timurkutluk B. *Ceramics International*[J], 2015, 41(2): 2057
- Macwan A, Marr M, Kesler O et al. *Thin Solid Films*[J], 2015, 584: 23
- Jian Shengrui, Lee Shengwei, Chang Jengkuei et al. *Science of Advanced Materials*[J], 2014, 6(8): 1691

## 等离子喷涂-物理气相沉积制备 7YSZ 纳米结构固体氧化物燃料电池电解质层

许伟<sup>1,2</sup>, 张小锋<sup>2</sup>, 周克崧<sup>1,2</sup>, 牛少鹏<sup>2</sup>, 常发<sup>3</sup>, 刘敏<sup>2</sup>, 邓春明<sup>2</sup>, 邓子谦<sup>2</sup>

(1. 中南大学, 湖南 长沙 410083)

(2. 广东省新材料研究所 现代材料表面工程技术国家工程实验室 广东省现代表面工程技术重点实验室, 广东 广州 510650)

(3. 福建工程学院, 福建 福州 350118)

**摘要:** 氧化钇稳定的氧化锆 (YSZ) 因其高热稳定性和良好的氧离子电导率被广泛地作为电解质材料应用于固体氧化物燃料电池 (SOFC)。本研究采用等离子喷涂-物理气相沉积 (PS-PVD) 技术成功地制备了致密的纳米结构 7YSZ 薄电解质层, 通过 SEM、TEM、工业 CT 以及纳米压痕等技术测定了 7YSZ 电解质层的微观形貌、结构、力学性能及气体透过率, 揭示了电解质层在沉积过程中的生长机制。结果表明: 基体温度是影响 7YSZ 电解质层纳米结构形成的关键因素; 当电解质层厚度为 8.7~12.3  $\mu\text{m}$  时, 其泄露率为  $2.24 \times 10^{-8} \sim 2.29 \times 10^{-8} \text{ cm}^4 \cdot \text{gf}^{-1} \cdot \text{s}^{-1}$ ; 同时, 7YSZ 电解质层还表现出良好的力学性能, 其硬度、弹性模量和弹性回复率分别为 10 GPa、140 GPa 和 57%。

**关键词:** 固体氧化物燃料电池; 氧化钇稳定的氧化锆; 物理气相沉积-等离子喷涂; 电解质层

---

作者简介: 许伟, 男, 1989 年生, 博士, 广东省新材料研究所, 广东 广州 510650, E-mail: xuw0907@163.com